

Partially-reflecting characteristic-based boundary conditions

R. Olsen¹, I. R. Gran²

¹Dept. of Energy and Process Engineering, NTNU, Norway, Robert.Olsen@sintef.no

²Dept. of Energy Processes, SINTEF Energy Research, Norway, Inge.R.Gran@sintef.no

Abstract

In characteristic-based boundary formulations, reflecting boundary conditions are used where non-reflecting boundary conditions are not applicable. Physical boundary conditions are set through the incoming wave amplitudes. This work propose to estimate the incoming wave amplitudes with control functions. The method which previous works have used, is identified as P-controllers. This study examines P- and PI-controllers for Poiseuille flow. A new test, which assesses the quality of the boundary conditions, is used to evaluate the boundary conditions. Results are found to improve significantly when a numerical filter is applied.

Introduction

Thompson [1, 2] presents a characteristic based way of developing boundary conditions for the Euler equations. This method is straightforward to implement, and to extend to other types of flow. Poinot and Lele [3] have developed this method further for direct numerical simulations of compressible flow, and Baum *et al.* [4] extend this to reactive multicomponent flow. Okong'o and Bellan [5] extend the method to real gas mixtures.

The key idea for characteristic-based boundary conditions (CBC) is to identify outgoing and incoming waves and then set the correct boundary conditions in terms of them. To ensure well posed and well behaved solutions, waves emerging from the computational domain must be calculated from the domain and not be specified. The CBC method is only strictly valid for hyperbolic systems, like the Euler equations. However, [3] use results from well-posedness analyses, extend CBC to the Navier-Stokes equations, and hence call it NSCBC (Navier-Stokes Characteristic Boundary Conditions). Characteristic-based boundary conditions have evolved to become an attractive way of solving the boundary problem, and have been used in a number of studies today.

Characteristic-based boundary conditions

A general system in three dimensions is treated as locally one-dimensional, where the normal direction to the boundary is denoted by x_1 . Terms from the other directions are passive in the analysis, meaning that the main effects of the flow are along the normal direction. To perform the analysis we need the primitive form of the equation system:

$$\frac{\partial U}{\partial t} + A \frac{\partial U}{\partial x_1} + C = 0. \quad (1)$$

Assume that A is diagonalizable, then a diagonal matrix, Λ , with the eigenvalues λ_i of A along the diagonal, can be obtained by the similarity transformation,

$$S^{-1}AS = \Lambda, \quad (2)$$

where $\Lambda_{ij} = 0$ for $i \neq j$ and $\Lambda_{ij} = \lambda_i$ for $i = j$. The columns of the matrix S are the right eigenvectors, r_j , and the rows of the inverse matrix, S^{-1} , are the left eigenvectors, l_i^T of A . Multiply

Eq. (1) with S^{-1} ,

$$S^{-1} \frac{\partial U}{\partial t} + S^{-1}A \frac{\partial U}{\partial x_1} + S^{-1}C = 0, \quad (3)$$

and define \mathcal{L} as,

$$\mathcal{L} \equiv \Lambda S^{-1} \frac{\partial U}{\partial x_1} \equiv S^{-1}A \frac{\partial U}{\partial x_1}, \quad (4)$$

This gives the primitive form of the *Time-dependent boundary conditions*:

$$\frac{\partial U}{\partial t} + S\mathcal{L} + C = 0. \quad (5)$$

If the system was linearly hyperbolic with $C = 0$ and A independent of U , then the change of variables to $W = S^{-1}U$, would give a set of wave equations,

$$\frac{\partial w_i}{\partial t} + \lambda_i \frac{\partial w_i}{\partial x} = 0, \quad (6)$$

with characteristic velocities λ_i . When $\lambda_i > 0$, the waves will propagate in the positive x -direction. It is then obvious that w_i cannot be specified at the right boundary, and that w_i must be specified at the left boundary. For a quasi-linear system like the Euler equations, it is not so simple anymore. However, it turns out that λ_i is the velocity and \mathcal{L}_i is the amplitude of the different waves and \mathcal{L}_i is the proper variable to specify at the boundary [1]. For outgoing^a waves the \mathcal{L}_i are calculated from its definition, Eq. (4). Therefore write the outgoing \mathcal{L}_i as \mathcal{L}_i^+ and incoming as \mathcal{L}_i^- . The eigenvector matrix S is also split into S^+ and S^- , where S^+ contains eigenvectors with positive eigenvalues. Eq. (5) now reads:

$$\frac{\partial U}{\partial t} + S^+ \mathcal{L}^+ + S^- \mathcal{L}^- + C = 0. \quad (7)$$

Since \mathcal{L}^- represents incoming waves, this is the only variable left to link the surroundings with the domain. Hence, all boundary conditions must be set through \mathcal{L}^- . The task is then to find equations for the unknown \mathcal{L}^- which represents different boundary conditions.

Typical boundary conditions for the generalised system

If the time-derivative of a given quantity, like for instance the velocity, is to be specified, an equation for \mathcal{L}_i^- may be found from Eq. (7),

$$S_i^- \mathcal{L}^- = - \left(\frac{\partial U_i}{\partial t} + S_i^+ \mathcal{L}^+ + C_i \right). \quad (8)$$

For a wall at rest the proper boundary condition would be to set the velocity equal to zero at the wall and find the \mathcal{L}_i^- which gives $\partial u / \partial t = 0$. Non-reflecting boundary conditions may be achieved by setting the amplitude of the incoming wave to zero, i.e. $\mathcal{L}_i^- = 0$. This may, however, in some cases lead to drifting

^aoutgoing means that $\lambda_i > 0$ at $x = x_{\max}$ and $\lambda_i < 0$ at $x = x_{\min}$.

values of the variable at the boundary and hence in the whole field. A way to overcome drifting values is to specify $\partial U_i/\partial t$ using a PID controller (three-mode controller):

$$S_i^- \mathcal{L}^- = (S_i^- \mathcal{L}^-)^\circ + \frac{K_P}{T} \Delta U_i + \frac{K_I}{T^2} \int_0^t \Delta U_i d\tau + K_D \frac{\partial U_i}{\partial t}, \quad (9)$$

where $\Delta U_i = (U_i - U_i^\infty)$, T is the integral time, K_P is the proportional gain, K_I is the integral gain, K_D is the derivative gain and a start term for the controller $(S_i^- \mathcal{L}^-)^\circ$. The start term can be based on an analytical solution, a previous simulation or simply set to zero. Inserting $\partial U_i/\partial t$ from Eq. (7) gives:

$$S_i^- \mathcal{L}^- = \text{PID}(U_i) \equiv \frac{1}{(1 + K_D)} \cdot \left((S_i^- \mathcal{L}^-)^\circ + \frac{K_P}{T} \Delta U_i + \frac{K_I}{T^2} \int_0^t \Delta U_i d\tau - K_D (S_i^+ \mathcal{L}^+ + C_i) \right). \quad (10)$$

The reasoning behind this method is presented in [6]. Now, the discussion continues with the Euler and the Navier-Stokes equations.

Single-phase Euler equations

The Euler equations in one-dimension reads:

$$\frac{\partial}{\partial t} (\rho) + \frac{\partial}{\partial x} (\rho u) = 0, \quad (11)$$

$$\frac{\partial}{\partial t} (\rho u) + \frac{\partial}{\partial x} (\rho u^2 + p) = 0, \quad (12)$$

and the equation of state

$$p = \rho c^2, \quad (13)$$

where c is the speed of sound.

Boundary matrices for the Euler equations

In this section, the boundary matrices for the Euler equations in one dimension, also referred to as the LODI (locally one-dimensional inviscid) relations are presented. The system vector, matrix and the eigenvalue matrix are

$$U = \begin{bmatrix} p \\ u \end{bmatrix}, \quad A = \begin{bmatrix} u & \rho c^2 \\ 1/\rho & u \end{bmatrix}, \quad \Lambda = \begin{bmatrix} u-c & 0 \\ 0 & u+c \end{bmatrix}. \quad (14)$$

The eigenvector matrix and the inverse

$$S = 1/2 \begin{bmatrix} 1 & 1 \\ -1/(\rho c) & 1/(\rho c) \end{bmatrix}, \quad S^{-1} = \begin{bmatrix} 1 & -\rho c \\ 1 & \rho c \end{bmatrix}. \quad (15)$$

When subsonic flow ($|u| < c$) is assumed, the eigenvector matrix at the upper boundary, ($x = x_{\max}$), is split into:

$$S^+ = 1/2 \begin{bmatrix} 1 \\ 1/(\rho c) \end{bmatrix}, \quad \text{and} \quad S^- = 1/2 \begin{bmatrix} 1 \\ -1/(\rho c) \end{bmatrix}. \quad (16)$$

We can also find \mathcal{L}^+ ,

$$\mathcal{L}^+ = \mathcal{L}_2 = (u+c) \left(\frac{\partial p}{\partial x} + \rho c \frac{\partial u}{\partial x} \right). \quad (17)$$

Non-reflecting boundary conditions

Eq. (5) now becomes:

$$\frac{\partial p}{\partial t} + \frac{1}{2} (\mathcal{L}_2 + \mathcal{L}_1) = 0, \quad (18)$$

and

$$\frac{\partial u}{\partial t} + \frac{1}{2\rho c} (\mathcal{L}_2 - \mathcal{L}_1) = 0. \quad (19)$$

\mathcal{L}_2 may be eliminated from the equations if we rewrite Eq. (19)

$$\mathcal{L}_2 = \mathcal{L}_1 - 2\rho c \frac{\partial u}{\partial t}, \quad (20)$$

and insert this in the pressure Eq. (18),

$$\frac{\partial p}{\partial t} - \rho c \frac{\partial u}{\partial t} + \mathcal{L}_1 = 0. \quad (21)$$

By setting $\mathcal{L}_1 = 0$, the non-reflecting boundary condition used by Rudy and Strikwerda [7] is found, see also the footnote on page 111 of Poinso and Lele [3].

It is known that specifying $\mathcal{L}_1 = 0$ may lead to a drifting pressure, and by studying Eq. (18) and Eq. (19) it is easy to realize why it happens. First note that a steady solution is only possible when $\mathcal{L}_2 = 0$, or $\partial p/\partial x = -\rho c \partial u/\partial x$. When using the Euler equations in 1D it is often the case that $\partial p/\partial x = \partial u/\partial x = 0$ in the steady solution and hence no drifting pressure will occur. A way to represent 2D viscous effects in a 1D-simulation is to use friction factors. By adding a wall friction term $f|u|u$ to Eq. (19), Eq. (21) now becomes:

$$\frac{\partial p}{\partial t} - \rho c \frac{\partial u}{\partial t} + \mathcal{L}_1 = \rho c f |u|u. \quad (22)$$

When $\mathcal{L}_1 = 0$ and $\partial u/\partial t = 0$ is specified at the other boundary, $\partial u/\partial t \rightarrow 0$ at this boundary as well. Eq. (22) is reduced to:

$$\frac{\partial p}{\partial t} = \rho c f |u|u. \quad (23)$$

It is now clear that the pressure will drift unless the velocity equals zero.

Partially reflecting boundary conditions

A way to overcome the problem of drifting pressure was proposed by [7]:

$$\frac{\partial p}{\partial t} - \rho c \frac{\partial u}{\partial t} + k(p - p_\infty) = 0, \quad (24)$$

where p_∞ is the pressure at some reference state located at infinity. [8] studied the behaviour of a linearised Navier-Stokes system and claimed that the coefficient k should be of the form $k = \sigma(1 - \mathcal{M}^2)c/L$. \mathcal{M} is the maximum Mach number in the flow, L is a characteristic size of the domain, and σ is a constant. They derived an optimal value for σ around 0.27, but their tests showed that a value of 0.58 provides better results. [3] compared Eq. (24) and several other methods, they arrived at setting $\mathcal{L}_1 = k(p - p_\infty)$ with $\sigma=0.25$ and using this in all equations at the boundary. They also suggested that the method might perform better if an analytical expression for \mathcal{L}_1 were available, then the expression for \mathcal{L}_1 becomes:

$$\mathcal{L}_1 = \mathcal{L}_1^{\text{exact}} + k(p - p_\infty). \quad (25)$$

If we consider the procedure of modifying Eq. (24) in terms of control engineering, the methods of the previous section are recognised as controllers. Specifically, the methods used by [7] and [3] are recognised as P-controllers for $\partial p/\partial t$.

It is known from control engineering that a PID-controller performs better than a P-controller. With $\Delta p = (p - p_\infty)$, a PID-controller for $\partial p/\partial t$ may be written as:

$$\mathcal{L}_1 = \frac{1}{1 + K_D} \left(\mathcal{L}_1^\circ + \frac{K_P}{T} \Delta p + \frac{K_I}{T^2} \int_0^t \Delta p d\tau - \frac{K_D}{2} \mathcal{L}_2 \right). \quad (26)$$

The P-controller of [3], Eq. (25), is found if we set $\mathcal{L}_1^\circ = \mathcal{L}_1^{\text{exact}}$, $K_P = kT$ and $K_I = K_D = 0$. [9] used the same approach as [3], at the inlet in addition to the outlet, i.e. by specifying \mathcal{L}_i^- on the form,

$$\mathcal{L}_i^- = K_{\text{in}}(u - u^\infty) + K_{\text{in}}(v - v^\infty). \quad (27)$$

Thus it makes sense to use a PID-controller at the inlet as well.

Numerical methods

For the time integration, the five-stage, fourth order, explicit Runge-Kutta scheme of [10] is chosen, mainly because it is nearly as effective as the standard RK-schemes while only needing two storage registers for each equation.

Finite differences (RKFD)

Eq. (1) is discretised in all points by replacing $\partial/\partial x$ by finite difference operators. After each time step, the solution vector U is filtered by a filter function,

$$\tilde{U} = (1 + \zeta_D D_f)U, \quad (28)$$

where the filter coefficient ζ_D is given by $(-1)^{n+1}2^{-2n}$ for a $(2n)$ th-order filter, and D_f is the dissipation matrix. Special care must be taken when $\partial U_i/\partial t$ is given on the boundary or estimated by a P-controller. The easiest solution is to not filter the boundary point for U_i . When a PID-controller is used at the boundary, there is no need for special care since the controller makes sure that the solution slowly converges to the specified value.

A more thorough discussion of explicit filters and high-order finite difference operators can be found in Kennedy and Carpenter [11].

Single-phase poiseuille flow

In order to check the implementation and to compare the different controlling methods, the plane channel of [3] is chosen.

Problem description

A viscous fluid, with kinematic viscosity $\nu = 2\text{m}^2/\text{s}$ and speed of sound $c = 300\text{m/s}$, flowing in a 2D plane channel, with length $L = 10\text{m}$ and half-height $h = 1\text{m}$, is studied here.

The inflow conditions are:

$$u(0, y, t) = u_0 \left[\cos\left(\frac{\pi y}{2h}\right) \right]^2, \quad (29)$$

$$v(0, y, t) = 0, \quad (30)$$

where $u_0 = 30\text{m/s}$ is the maximum inlet velocity. The Reynolds number is $Re = u_0 h/\nu = 15$ and the Mach number is $\mathcal{M} = u_0/c = 0.1$. An analytical solution may be found if this case is considered to be incompressible. A criterion for this is:

$$\frac{L}{h} \frac{\mathcal{M}^2}{Re} \ll 1. \quad (31)$$

For this computation, $L/hRe^{-1}\mathcal{M}^2 = 0.007$ and the incompressible solution may be considered to be close to the exact one. The exact solution is:

$$\frac{\partial p^e}{\partial x} = -\frac{3}{2}Re^{-1}\rho u_0^2, \quad (32)$$

where

$$u(x, y, t) = u_m(1 - (y/h)^2), \quad (33)$$

and u_m is the maximum velocity: $u_m = -\frac{1}{2\mu} \frac{\partial p^e}{\partial x} h^2$. Initial values for the calculations are:

$$\begin{aligned} u(x, y, 0) &= u_0 \left[\cos\left(\frac{\pi y}{2h}\right) \right]^2, \\ v(x, y, 0) &= 0, \\ \rho(x, y, 0) &= \rho_{\text{in}} = 1\text{kg/m}^3. \end{aligned} \quad (34)$$

At the inlet, the velocity is specified and the unknown \mathcal{L}_i are found from the LODI relations, (Sec.). At the outlet, the pressure is specified with a controller for $\partial p/\partial t$. For simplicity, the discussion is restricted to P- ($K_I = K_D = 0$) and PI-controllers ($K_D = 0$ in Eq. (26)):

$$\mathcal{L}_1 = \mathcal{L}_1^\circ + K_P \Delta p + \frac{K_I}{T} \int_0^t \Delta p d\tau, \quad (35)$$

$$\mathcal{L}_1^\circ = (u - c) \left(\frac{\partial p^e}{\partial x} - \rho c \frac{\partial u^e}{\partial x} \right), \quad (36)$$

where $\partial u/\partial x^e$ is found from continuity of the exact solution. For the proportional term we take $K_P = \sigma(1 - \mathcal{M}^2)c/L$ and the integral term is $K_I = K_P$.

About the computations

The Navier-Stokes equations were discretised in the same manner at the boundary as in the inner domain. The domain was discretised with an equidistant 21×21 grid and the spatial discretisations were obtained with an eight-order first-derivative operator. For the viscous terms, the first-derivative operator was applied twice. The solution was filtered after each time step with an eight-order explicit filter. The steady-solution found agrees with [3].

Evaluation of the boundary conditions

In order to find out how good the boundary conditions are, they should be tested where something can be stated about their performance. Therefore a new test for the boundary conditions is presented.

In Fig. 1 three Channels A, B and C are shown, for clarity the figure is not drawn dimensionally correct. The length of Channel C in Fig. 1 is twice that of Channel A and Channel B. With this configuration, the obtained solution in Channel A can be compared with the solution in the first part of Channel C, and logically the solution obtained in Channel B can be compared with the solution in the second part of Channel C.

This test can be done since the PI-controllers have the ability to specify the pressure to any degree of accuracy. Note that to perform this test with a P-controller would be cumbersome, since it would require an iteration procedure to specify the pressure to a high degree of accuracy.

This approach will give an idea of the performance of the boundary conditions, furthermore it is even possible to extract approximate values of \mathcal{L}_i at $x = L$ from Channel C and compare them with the values for Channel A and B. Here, however, the discussion is restricted to comparing the converged solution for the three cases.

Boundary conditions for Channel C: The same channel as earlier in this section is calculated, but now with length $2L$. The boundary conditions are the same as before, specifying the outlet pressure p_∞ with a PI-controller and setting the inlet velocity.

Boundary conditions for Channel A: To compute the first part of the channel, the same boundary conditions as for Channel C

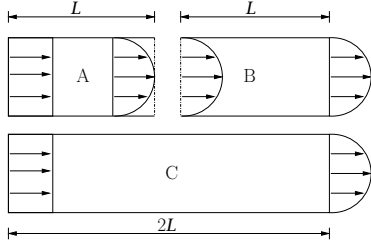


Figure 1: Test case for evaluating the boundary conditions.

were used, except that the pressure $p_L = p_{x=L}$ obtained at $x = L$ from Channel C was specified instead of p_∞ .

Boundary conditions for Channel B: A natural choice would be to specify boundary conditions for Channel B as for Channel A and Channel C. That is by reading the velocity profile at $x = L$ in Channel C, and specify this at the inlet. However, this way of specifying boundary conditions is already tested for Channel A. Since the flow in Channel B is fully developed, boundary conditions for fully developed flow can be tested instead.

For the second part of the channel, a PI-controller was applied for the pressure at both the inlet and outlet, i.e. specifying p_L at the inlet and p_∞ at the outlet. According to theory, one more boundary condition must be specified at the inlet, so a P-controller for the v -velocity was used.

This problem was computed with the RKFD approach and gave excellent results. In order to compare and quantify the error, the relative difference between the simulations has been calculated. The relative error is defined by:

$$e(f) = \left| \frac{f_{2L} - f_L}{f_{2L}} \right|, \quad (37)$$

where f_{2L} is evaluated in Channel C. f_L is evaluated in Channel A when $0 \leq x \leq L$ and in Channel B when $L \leq x \leq 2L$. The error is computed in all points, except where f_{2L} is zero. To simplify the comparisons, it makes sense to use the maximum of $e(f)$ as a measure of performance.

In Tab. 1, Channel A and C are compared for three computations. The first column tells which variable is compared, and the second column at which point the comparison is done. For instance (mx,2) is at the maximum in x -direction and point 2 in the y -direction. In the next column, the label 2x-8f means that the spatial derivative operator is second-order, and the filter is eight-order.

The first to be read from the table is that the error goes significantly down when filtering is applied, and slightly down when the order of the spatial operator is increased. Second, when the error in the u -velocity is as low as $1 \cdot 10^{-5}$ it is for most practical purposes zero. It is then reasonable to conclude that a filter should be applied when available. This is confirmed when the grid resolution is increased, since then the computations were unstable when filtering was not applied.

When comparing Channel B and C, similar results as when comparing Channel A and C are obtained.

Concluding remarks

Characteristic based boundary conditions have been reviewed for single-phase flow. The method of avoiding a drifting pressure has been analysed, and this method turns out to be the implementation of a control function for estimating the incoming wave amplitude.

Table 1: Comparison of Channel A and C for the RKFD computations

$e(f)$	(i, j)	2x-NO	2x-8f	8x-8f
u	(mx,2)	0.0031	$9.6 \cdot 10^{-5}$	$6.45 \cdot 10^{-5}$
u	(2,2)	0.0013	$1.8 \cdot 10^{-5}$	$1 \cdot 10^{-5}$
p	any	$12 \cdot 10^{-7}$	$4.3 \cdot 10^{-7}$	$9 \cdot 10^{-8}$

The hypothesis of the use of control functions has been tested for single-phase, and been verified.

Particularly P- and PI-controllers have been tested with different arrangements. When the start term for the controller was zero, the P-controller gave the best convergence. However, it was not able to specify the imposed value. The PI-controller made it possible to specify a given value. Based on this the PI-controller was preferred. The case when the PI-controller have been used to set the inlet as well as the outlet had better performance in the tests, except on convergence. The case where the inlet values are set directly had almost as good results as the others. Therefore, setting the inlet values directly may in some cases be the best choice.

This work has been sponsored by the Research Council of Norway. *

References

- [1] Thompson K.W. Time-dependent boundary conditions for hyperbolic systems. *Journal of Computational Physics* 68 (1) (1987) 1–24.
- [2] Thompson K.W. Time-dependent boundary conditions for hyperbolic systems. II. *Journal of Computational Physics* 89 (2) (1990) 439–461.
- [3] Poinso T.J., Lele S.K. Boundary conditions for direct simulations of compressible viscous flows. *Journal of Computational Physics* 101 (1992) 104–129.
- [4] Baum M., Poinso T., Thévenin D. Accurate boundary conditions for multicomponent reactive flows. *Journal of Computational Physics* 116 (1994) 247–261.
- [5] Okong'o N., Bellan J. Consistent boundary conditions for multicomponent real gas mixtures based on characteristic waves. *Journal of Computational Physics* 176 (2002) 330–344.
- [6] Olsen R., Gran I.R. Estimation of incoming wave amplitudes for characteristic-based boundary conditions. Submitted to *Journal of Computational Physics*.
- [7] Rudy D.H., Strikwerda J.C. A nonreflecting outflow boundary condition for subsonic Navier-Stokes calculations. *Journal of Computational Physics* 36 (1980) 55–70.
- [8] Rudy D.H., Strikwerda J.C. Boundary conditions for subsonic compressible Navier-Stokes calculations. *Computers & Fluids* 9 (1981) 327–338.
- [9] Kim J.W., Lee D.J. Generalized characteristic boundary conditions for computational aeroacoustics. *AIAA Journal* 38 (11) (2000) 2040–2049.
- [10] Carpenter M., Kennedy C. Fourth-order 2n-storage runge-kutta schemes. Tech. Rep. NASA TM-109112, Langley Research Center, Hampton, VA, 1994.
- [11] Kennedy C.A., Carpenter M.H. Several new numerical methods for compressible shear-layer simulations. *Applied Numerical Mathematics* 14 (1994) 397–433.